Study on Preparation of Autoclaved Aerated Concrete Using Lead-Zinc Tailings

Changlong Wang[a,b,c], Zhenyu Liu[a], Jun Li[a*], Shenhua Jiao[d], Yuyan Zhang[e]

[a]School of Civil Engineering, Hebei University of Engineering, Handan 056038, China

[b]Jiangxi Key Laboratory of Mining Engineering, Jiangxi University of Science and Technology, Ganzhou 341000, China

[c]Tianjin Sunenergy Sega Environmental Science & Technology Co. Ltd, Tianjin 300000, China

[d]China Ordnance Industry Survey and Geotechinical Institute, Beijing 100053, China

[e]China Center for Information Industry Development of MIIT Institute of Industry Energy Conservation and Environment Protection, Beijing 100846, China

9195922@qq.com

For comprehensive utilization of solid wastes, the autoclaved aerated concrete (ACC) were prepared by using lead-zinc tailings (LZT) as mainly siliceous materials. The effects of fineness and dosage of LZT on the AAC properties, hydration products and microstructures of AAC were analyzed by the mechanical test, X-ray diffraction analysis (XRD) and scanning electron microscope (SEM). The results show that the ACC containing 62 % LZT (in mass percentage) with a surface area of 325 m^2 kg^{-1} (grinding time of 25 min) can achieve a bulk density of 587 kg m^{-3} and compressive strength of 4.94 MPa, which is in line with the requirement of A3.5, B06-class AAC products regulated by *autoclaved aerated concrete building blocks (GB/T 11969-2008)*. The mobility of slurry and hydration activity increase with decreasing fineness of LZT. However, the small size of LZT powder and high thickness of the slurry are bad to form good pore structure, which would influence the properties of AAC. When the blending percentage of LTZ is too high, the unreacted LTZ particles increase and accumulate within the system, which reduces the space among them and thus influences the growth and crystallization of hydration products. The main hydration products in the AAC are C-S-H gels and tobermorite-11 Å.

1. Introduction

Autoclaved Aerated Concrete (AAC) is a cellular building materials, which provides high thermal efficiency, superior fire resistance and excellent acoustical absorbing abilities (Cui et al., 2017). It can be used as a substitution for fired clay brick with the benefits for farmland conservation, environmental protection, and energy saving. The basic ingredients of AAC are calcareous materials (cement and lime) and siliceous materials (silica sand or recycled fly-ash), and an expansion agent—aluminum powder. In some areas, the shortage of high silica content sand limited the production and application of AAC. However, there is a large amount of silica in metal ore mining. That is the reason why lead-zinc tailings (LZT) was chosen for the present application. LZT which is formed by dehydrated ore pulp which comes from the process of sorting tailings is the main types of industrial solid waste (Wang 2001). LZT are a kind of concomitant mine, associated with a variety of heavy metals, non-metallic minerals and other hazardous substances. The metal resources of LZT are difficult to recover so that the plant usually stored the LZT by stockpiling, which occupies a large amount of arable land, causes serious pollution to the surrounding environment and seriously affects the sustainable development of mining area. The obtained fine LZT particles contain by crushing, grinding and milling contains large amounts of silicate minerals, and it has different physical and chemical properties compared with conventional acidic material used to produce AAC materials, such as fly ash and river sand (Torsten, 2004). The active components in silicate minerals such as Al_2O_3 and SiO_2, are prone to carry on hydration reaction in alkaline hydrothermal environment at high temperature and high pressure, and produce hydrate calcium silicate hydrates (C-S-H) (Tian et al., 2006). There have been successful have been successfully applied in AAC production in China by metal mining tailings with large amounts of silicate

minerals such as iron ore tailings and gold tailings. Also, some mining companies and research institutes are trying to use copper tailings, phosphorus tailings and other tailings to produce AAC. Only Zhang, (2012), Chen (2009) and Li et al., (2008) studied the preparation of AAC in B05, B06 level with LZT, but the dosage of LZT was low and the consumption of mixing cement was more than 18% in the preparation of AAC process, besides the analysis on the reaction mechanism of LZT AAC was not carried out. In this paper, LZT will be used as the main raw materials in AAC with as little amount of cement. The effects of grinding and dosage of LZT and pre-curing temperature on the AAC properties, hydration products of ACC were investigated by the mechanical test, XRD and SEM.

2. Experimental

2.1 Raw Materials Characteristics

The AAC samples were prepared using the following raw materials: LZT, lime (L), 42.5 ordinary Portland cement (OPC) and the gypsum of flue gas desulfurization waste (FGDW). The chemical compositions of the raw materials are listed in Table 1.
OPC. The cement used was ordinary Portland cement with the strength grade of 42.5 which complies with the Chinese National Standard GB 175–1999. The chemical compositions and the physical properties of OPC are shown in Table 1 and Table 2, respectively.
LZT. Table 1 shows that the amount of SiO_2 in the LZT was approximately 68.96 %, leaching toxicity of heavy metals in LZT accordance with Chinese Standard GB/T 5085.3-2007, "*Standard of Hazardous Waste Identification—leaching toxicity identification*" and the radioactivity accordance with Chinese Standard 6566-2010, "*Limit of radionuclides in building materials*". The remainder is 66.41% after LZT screened with a 0.08 mm square holes sieve.
L. The composition of lime is shown in Table 1and the content of effective CaO is 71%. Its digestion time is 12 min, and the digestion temperature is 67 ºC according to Chinese standard JC/T621-1996. And 0.08 mm sieve residue is less than 15%.
FGDW. Its chemical compositions are listed in Table 1.The specific surface area (SSA) of FGDW is 200 m^2 kg^{-1}, and 0.08 mm sieve residue is less than 7.9 %.

Table 1: Chemical composition of raw materials (mass fraction, %)

Materials	SiO_2	Al_2O_3	Fe_2O_3	FeO	CaO	MgO	Na_2O	K_2O	SO_3	MnO	Loss
LZT	66.23	7.67	2.45	3.12	8.51	1.78	0.54	0.65	—	4.13	3.83
L	4.79	4.32	3.21	0.48	76.89	2.96	—	1.63	0.53	—	4.18
OPC	26.12	5.75	3.17	0.93	57.29	1.53	0.54	0.31	—	0.12	4.02
FGDW	2.64	0.84	0.08	0.22	43.65	0.14	0.21	0.23	31.16	—	—

Table 2: Physical properties of cement

Fineness(residue on 80 µm sieve) /%	Normal consistency /%	Setting time /min		Stability	Flexural strength /MPa		Compressive strength /MPa	
		Initial setting	Final setting		3 d	28 d	3 d	28 d
22.13	27.20	160	220	qualified	5.3	8.8	32.5	59.7

2.2 Experimental Method

2.2.1 Preparation of AAC
Firstly, LZT and FGDW were dried in oven (DH-101) at 105 ºC for 24 h to make moisture content less than 1 wt.%, Then they were grinded with the SM Φ500 mm×500 mm 5 kg small ball grinder at the speed of 48 r·min^{-1}. The grinding periods of LZT were chose at 15 min, 20 min, 25 min, 30 min, 35 min and 40 min in order to obtain different surface area. According to the grinding periods, the obtained ground samples were labeled as G_{15}, G_{20}, G_{25}, G_{30}, G_{35}, G_{40}, respectively. FGDW was also grinded to a SSA of 380 m^2 kg-1.
(1) Preparation of AAC containing LZT with varying grinding time
The amounts of LZT, OPC, L, and FGDW are 1320 g, 550 g, 220 g, 110 g, respectively. And the amounts of water, aluminum paste and foam stabilizer are 1254 g, 1.32 g and 0.56 g, respectively. The dry mixtures were stirred in warm water (50 ºC) for 120 s; then added aluminum paste and foam stabilizer and continued to stir the mixtures for 40s. The slurry was poured into the triple-mold molds (100mm×100mm×100mm), then cured at 60 ºC for 4 h. After de-molded, the hardened slurries were autoclaved for 8 h (the highest pressure is 12.5

bars, and the highest temperature 185 ºC). The different LZT fineness of AAC samples were labeled as Z_1, Z_2, Z_3, Z_4, Z_5 and Z_6.

(2) The preparation of AAC with different dosage of LZT

LZT with the optimal fineness was used and its blend amounts are as follows: 1188 g, 1232 g, 1276 g, 1320 g, 1364 g, 1408 g and 1452 g. At the same time, adjusted the amount of OPC, L and FGDW. Then, the different LZT dosage of AAC samples were labeled as C_1, C_2, C_3, C_4, C_5 and C_6. The amount of water, aluminum powder pastes and foam stabilizer were the same as before. Meanwhile, the process of preparation was also the same as before.

2.2.2 Sample characterisation

The particle size distribution of ground LZT was analyzed using laser particle size analyzer (MASTER SIZER 2000, the analysis range was 0.02~2000.00 μm) with ethanol as the dispersant. The SSA of LZT was measured using dynamic SSA analyzer (SSA-3200). The bulk density and compressive strength of the AAC samples were measured according to Chinese standard GB/T 11968-2008 *Autoclaved aerated concrete blocks.* The strength of AAC samples were measured using hydraulic pressure testing machine (YES-300) with a maximum load of 300 KN and a loading rate of 2.0±0.5 kN/s. The X-ray diffraction (XRD) spectra of AAC samples were performed using a D/Max-RC diffractometer (Japan) with Cu Kα radiation, voltage of 40 kV, current of 150 mA and 2θ scanning ranging between 5 ° and 90 °. SEM observation was performed to analyze the microstructure of samples using a Zeiss SUPRA^{TM}55 scanning electron microscope coupled with a Be4-U92 energy spectrum.

3. Results and discussion

3.1 Effect of the fineness of LZT on AAC properties

According to Figure 1, the particle size decreases rapidly after 15 min of powder grinding, leaving over 50% of particles smaller than 10 μm. As the powder grinding persists, fewer and fewer particles remain larger than 10 μm. It was shown that LZT particles were gradually refined during the powder grinding process, and the increasing of the grinding time promotes the decrease of the LZT particle size.
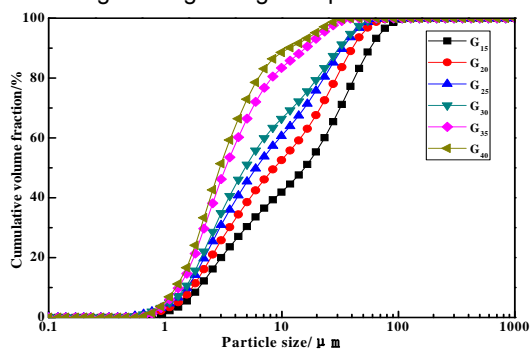

Figure 1: Relationship of particle size distribution and grinding time.

As can be seen from Table 3, the D_{10}, D_{50} and D_{90} of LZT particle size distribution declined with the increasing of grinding time. Specifically, D_{10} dropped from 1.950 μm to 1.234 μm, D_{50} dropped from 15.770 μm to 2.933 μm, and D_{90} dropped from 57.090 μm to 11.553 μm. The downward trend testified the gradual increasing of fine particles and decrease of large particles as the grinding time prolongs.

Table 3: SSA and characteristic particle size of LZT in different grinding time periods

Grinding time/min	SSA/(m^2 kg^{-1})	Characteristic particle size /μm		
		D_{10}	D_{50}	D_{90}
G_{15}	210	1.950	15.770	57.090
G_{20}	275	1.709	8.633	40.196
G_{25}	325	1.544	6.028	33.203
G_{30}	360	1.486	5.839	30.9081
G_{35}	385	1.300	3.289	15.951
G_{40}	405	1.234	2.933	11.553

Table 3 showed the SSA of the samples of G_{15}, G_{20}, G_{25}, G_{30}, G_{35} and G_{40} were respectively 210 m^2 kg^{-1}, 275 m^2 kg^{-1}, 325 m^2 kg^{-1}, 360 m^2 kg^{-1}, 385 m^2 kg^{-1} and 405 m^2 kg^{-1} respectively. The SSA of LZT increased rapidly

at the early stage of grinding. The grinding time was from 15 min to 25 min, and the SSA was increased by 41.67 %. However, the grinding time increased from 25 min to 30 min, and the SSA only increases by 9.72 %. Due to the phenomenon of weak agglomeration in grinding 25 min, the SSA changed little, which corresponds to the change of particle size distribution (See Figure 1). Meanwhile, the grinding time was from 25 min to 30 min, and the characteristic particle size of D_{10} decreased by 0.058 μm, D_{50} only decreases by 0.189 μm. Therefore, in terms of energy conservation and cost, LZT used in this study should be controlled at 25 min grinding time when used as the siliceous materials in the AAC production.

Table 4: Effect of fineness of LZT on the casting stability and properties of AAC samples

SSA/(m^2 kg^{-1})	Samples number	Slurry fluidity	Casting stability	Bulk density/($kg \cdot m^{-3}$)	Compressive strength /MPa
210	Z_1	poor	bubbling	602	3.38
275	Z_2	general	good	593	4.15
325	Z_3	good	good	585	4.81
360	Z_4	good	preferably	586	4.55
385	Z_5	preferably	preferably	598	4.38
405	Z_6	preferably	slightly bubbling	613	4.04

As can be seen from the Table 4, with the fineness of LZT decreasing, compressive strength of AAC samples increased first and then decreased, but its bulk density tended to decrease first and then increase. Bulk density of six group samples were smaller than 625 kg m^{-3}, which met requirement of Chinese standard B05 AAC. And compressive strength of Z_2, Z_3, Z_4, Z_5, Z_6 samples was all higher than 3.5 MPa, which met the requirement of Chinese standard A3.5 AAC, but compressive strength of Z_1 sample was 3.38 MPa, which could not reach standard. Thus the fineness of LZT was very important for properties of AAC. Like cement and other cementitious materials, the tailings surface area in contact with water could be increased by improving the fineness. The new produced surface crystal was ground to break and became amorphous, which improved the rate of dissolution, enhance the ability of materials to participate in the chemical reaction and stimulate tailings activity. Slight bubbling phenomenon was found in the sample slurry Z_6 with specific surface area of 405 m^2 kg^{-1} in the experiment. The hydration products was very viscous and of poor products appearance. This indicated that the smaller fineness of LZT was, the larger surface area of the particles participating in the reaction was, the higher the activity was, the better the flow of slurry was; however, when the fineness of the particles was too small and the slurry was too thick, hydration products could not form a good pore structure and the performance of the samples were affected; Z_1 sample with specific surface area of 207 m^2 kg^{-1} showed poor flow properties of the slurry and bubbling phenomenon was found, which indicated that if LZT was coarse, fineness was too large and poor flow properties of the slurry. Settlement became fast after pouring, which easily lead to the collapse of the mold and subsidence phenomenon. The experimental results showed that when specific surface area of tailings was 325 m^2 kg^{-1}, liquidity and pouring stability of the slurry were good, bulk density and compressive strength enhancement of samples were optimal and appearance of AAC samples was best. Therefore, considering from the economic and properties, the optimal specific surface area of the following test tailings was determined to be 325 m^2 kg^{-1}.

3.2 Effect of the dosage of LZT on AAC properties

As can be seen from Figure 2, with the increasing dosage of LZT, compressive strength of AAC samples overall tended to increase first and then decrease, bulk density tended to increase after the first reducing. With the dosage of LZT increasing, the amount of dissolved active SiO_2 and Al_2O_3 increased, hydration reaction conducted completely in system, crystal morphology of hydration products (tobermorite) was good in alkaline conditions. Hydration products combined more closely with unreacted particles in the system, which increased the compressive strength of AAC samples and decreased the bulk density. But when mixed with excessive LZT, residual unreacted particles of tailing in the system increased, the space among the particles were reduced, which was not conducive to the growth and crystalline hydrates and made crystalline of hydrates become poor so that compressive strength reduced and bulk density increased (Bensted and Barnes, 2001). When the dosage of LZT was 1408 g and 1452 g, the excessive iron tailings made slurry liquidity decrease, the initial consistency of the slurry increase, pore structure uneven in body, expanded height of body decrease, the compressive strength reduce and the pore structure of hydration products uneven. When the dosage of LZT was 1452 g (C_7 sample), the outer surface appeared a small amount of vertical hairline cracks, which indicated that dosage of LTZ could not be larger than 1364 g under the experimental conditions and when the dosage of the LZT was 1364 g, absolute bulk density of sample was 587 kg m^{-3} and compressive strength could reach 4.94 MPa. Considering the samples properties, making the most use of LZT, and

reducing costs, the C$_5$ sample (LZT of 1364 g, L of 528 g, OPC of 198 g, FGDW of 110 g) was determined to be the best proportion.
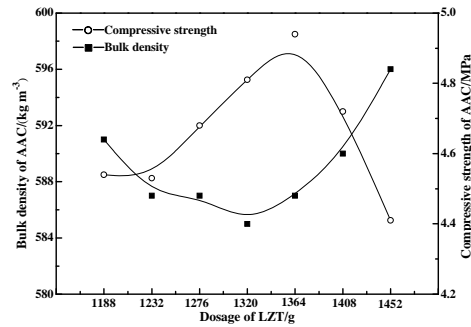

Figure 2: Influence of LZT dosage on AAC samples properties.

3.3 Phase composition and microstructure analysis of LZT AAC

The curve of original LZT in Figure 3 identified that most of the minerals were well crystallized, which suggested by the sharp diffraction peaks and low back ground. The main minerals phases were quartz (SiO_2), johannsenite (calcium manganese pyroxene, $CaMn(SiO_3)_2$), hedenbergite ($CaFe(Si_2O_6)$), diopside ($CaMg(Si_2O_6)$), calcite ($CaCO_3$) and epidote ($Ca_2FeAl_2[SIO_4][SI_2O_7]O(OH\ )$). It can be seen that the major minerals in the final AAC sample were tobermorite-11 Å, anhydrite, johannsenite, hedenbergite, diopside, calcite, epidote and residual minerals quartz. Comparing spectra of LZT and AAC, the characteristic peaks of quartz decreased significantly. That was to say the minerals in IOT was evidently involved into the hydrothermal reaction during the 8 h autoclaving process. AAC Body autoclaved beginning stages, the insufficient amount of dissolved Si^{4+} ions and Al^{3+} ions from LZT were present with an excessive amount of $Ca(OH)_2$, resulting in the formation of a small amount of tobermorite-11 Å (Zhang et al., 2016). (Wang et al., 2016). As the autoclaving time extended, a large amount of Si^{4+} ions and Al^{3+} ions were dissolved from LZT in alkaline hydrothermal conditions, which promoted the formation of tobermorite. At the same time, the broad band at around of "convex closure" in two theta range between 26–34 ° indicated that there is amorphous diffraction (no) of amorphous and low crystallized C-S-H gels (Bensted and Barnes, 2001). And diffraction peak intensity of the anhydrite in Figure 3 is strengthened after curing due to the delayed coagulation of FGDW. The anhydrite with non-reacted johannsenite, hedenbergite, diopside, calcite, epidote and residual minerals quartz would become the primary aggregate in the AAC samples.
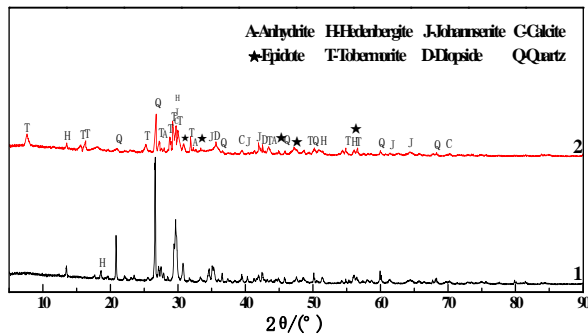

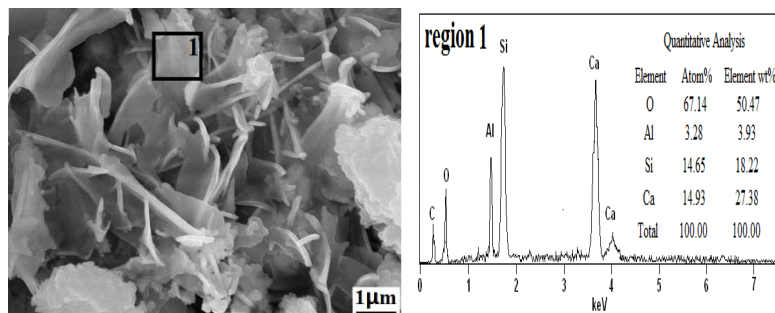Figure 3: XRD spectra of C5 AAC sample and LZT: 1-LZT; 2- AAC sample.

Figure 4: SEM and EDS spectra of C5 AAC sample.

As shown in Figure 4, the main hydration products in C5 sample after autoclaved for 12 h include C-S-H with a high degree of crystallinity and plate-shaped hydrates. The EDS spectra of region 1 in Figure 4 showed that Al existed in the plate-shaped tobermorite due to the partial substitution of $[SiO_4]$ by $[AlO_4]$. Hydration products in the area 1 $nCa/n(Si+Al)=0.8326$ can be obtained, which is the same as that of tobermorite $(Ca_5(OH)_2Si_6O_{16}!4H_2O)$ $n(Ca)/n(Si)=0.8333$. And this was consistent with the XRD (Figure 3) analysis. C-S-H gels and tobermorite intertwined together to forming the skeleton structure of AAC products, which contributed to the strength of AAC. After autoclaved, the solubility of active SiO_2 and Al_2O_3 in LZT increased in alkaline water heat environment and ability to participate in chemical reactions enhanced, which played a positive role in improving the crystallinity of hydration products.

4. Conclusions

(1) As the fineness of LZT decreases, the bulk density and compressive strength of the AAC increases. However, extra fineness may weaken those properties. With the decreasing fineness of LZT, the specific contact surface area between tailings and water increases, which adds SiO_2 solubility, makes it easier for tobermorite to crystallize and thus strengthens the products. However, extra fineness may cause the size of unreacted residues to become too small, where tobermorite crystallizes badly, failing to provide a good structure for products. Thus the bulk density increases and the compressive strength decreases.
(2) As the LZT dosage increases, the amount of dissolved active SiO_2 and Al_2O_3 increases in the system, and the hydration reaction tends to complete. Thus, the physical and mechanical properties of AAC samples enhances. But when mixing with excessive LZT, residual and the amount of unreacted LZT increases in the system. The space among the particles reduces, which restrains the growth and crystallization of hydration products, resulting in the degradation of products.
(3)The strength of AAC is obtained from the cemented combination of the unreacted materials and tobermorite and C-S-H gels that are formed by the reaction between the positive components, namely SiO_2 and Al_2O_3, and lime, cement, and other materials.

Reference

Bensted J., Barnes P., Buenfeld N.R., Eds., 2001, Structure and performance of cements, 2nd edition. Spon Press, Oxford, UK.

Chen J., 2009, The preparation and thermal analysis for B05 autoclaved aerated concrete. Wuhan University of Technology, Wuhan, China.

Cui X.W., Wang C.L., Ni W., Di Y.Q., Cui H.L., Chen L., 2017, Study on the reaction mechanism of autoclaved aerated concrete based on iron ore tailings, Romanian Journal of Materials, 47(3), 46-53 (in Romania).

Li F.X., Chen Y.Z., Long S.Z., Experimental investigation on autoclaved aerated concrete with addition of lead-zinc tailings, Journal of Southwest Jiaotong University 43, 810-815 (in China).

Tian X.F., Zhang D.J., Hou H.B., Yang Z.B., Liu H., 2006, Microstructure of weak soil stabilization slag cementing material, Journal of the Chinese Ceramic Society, 34(5), 636-640 (in China), DOI: 10.14062/j.issn.0454-5648.2006.05.026.

Wang C.L., Ni W., Zhang S.Q., Wang S., Gai G.S., Wang W.K., 2016, Preparation and properties of autoclaved aerated concrete using coal gangue and iron ore tailings, Construction and Building Materials, 104(1), 109-115, DOI: 10.1016/j.conbuildmat.2015.12.041.

Wang Y.P., 2011, Empirical study of system management of lead-zinc tailings in Shaoxing Yinshanfan, Hangzhou Dianzi University, Hangzhou, China.

Zhang W.Q., 2012, Research on preparation and property of tungsten tailings aerated concrete. Nanchang University, Nanchang, China.